Saudi Journal of Biological Sciences 28 (2021) 2581–2590

Contents lists available at ScienceDirect

Saudi Journal of Biological Sciences

journal homepage: www.sciencedirect.com

Original article

MicroRNA-567 inhibits cell proliferation and induces cell apoptosis in A549 NSCLC cells by regulating cyclin-dependent kinase 8

Mohamed A. Elkady [a,*], Ahmed S. Doghish [a,b,*], Ahmed Elshafei [a], Mostafa M. Elshafey [a]

[a] Department of Biochemistry and Molecular Biology, Faculty of Pharmacy (Boys), Al-Azhar University, Nasr City, Cairo 11651, Egypt
[b] Department of Biochemistry, Faculty of Pharmacy, Badr University in Cairo (BUC), Badr City, Cairo 11829, Egypt

ARTICLE INFO

Article history:
Received 29 December 2020
Revised 31 January 2021
Accepted 1 February 2021
Available online 14 February 2021

Keywords:
Apoptosis
CDK8
Cell cycle
Cell proliferation
MiR-567
NSCLC

ABSTRACT

MicroRNA-567 (miR-567) plays a decisive role in cancers whereas its role in non-small cell lung cancer (NSCLC) is still unexplored. This study was therefore planned to explore the regulatory function of miR-567 in A549 NSCLC cells and investigate its possible molecular mechanism that may help in NSCLC treatment. In the current study, miR-567 expression was examined by quantitative real time-polymerase chain reaction (qRT-PCR) in different NSCLC cell lines in addition to normal cell line. A549 NSCLC cells were transfected by miR-567 mimic, miR-567 inhibitor, and negative control siRNA. Cell proliferation was evaluated by MTT and 5-bromo-2′deoxyuridine assays. Cell cycle distribution and apoptosis were studied by flow cytometry. Bioinformatics analysis programs were used to expect the putative target of miR-567. The expression of cyclin-dependent kinase 8 (CDK8) gene at mRNA and protein levels were evaluated by using qRT-PCR and western blotting. Our results found that miR-567 expressions decreased in all the studied NSCLC cells as compared to the normal cell line. A549 cell proliferation was suppressed by miR-567 upregulation while cell apoptosis was promoted. Also, miR-567 upregulation induced cell cycle arrest at sub-G1 and S phases. CDK8 was expected as a target gene of miR-567. MiR-567 upregulation decreased CDK8 mRNA and protein expression while the downregulation of miR-567 increased CDK8 gene expression. These findings revealed that miR-567 may be a tumor suppressor in A549 NSCLC cells through regulating CDK8 gene expression and may serve as a novel therapeutic target for NSCLC treatment.

1. Introduction

Lung cancer (LC) is the greatest widespread cancer throughout the world. The GLOBOCAN reported 2.09 million new LC cases and 1.76 million LC deaths in 2018 (Krishnamoorthy and Vilwanathan, 2020). Non-small cell lung cancer (NSCLC) is the highest LC type representing 85% of all LC cases (Liu et al., 2019). Among which 50% are adenocarcinoma, the major histological subtype of NSCLC (Yoshimura et al., 2019). Despite recent advances in diagnostic methods, NSCLC is mostly diagnosed in late stages, and the survival rate of this disease is very dismal (Zhu et al., 2016). As well, the therapeutic strategies for NSCLC treatment have been improved. Nonetheless, the prognosis of NSCLC disease is still very poor (Zhang et al., 2017).

Regardless the availability of several treatment modalities, these modalities are still suboptimal and the curative treatment for NSCLC is still unmet pressing medical necessity (Lemjabbar-Alaoui et al., 2015). The progress of optimal therapeutics for NSCLC

Abbreviations: ATCC, American type culture collection; BrdU, 5-bromo- 2′-deoxyuridine; CDK8, Cyclin-dependent kinase 8; cDNA, Complementary DNA; DAPI, 4′, 6-Diamidino-2 Phenylindole, Dihydrochloride; DMEM, Dulbecco's modified Eagle's medium; DMSO, Dimethyl sulfoxide; FBS, fetal bovine serum; FITC, Fluorescein isothiocyanate; 16HBE, Normal human bronchial epithelial cell line; h, Hour; LC, Lung cancer; MiR or MiRNA, MicroRNA; mRNA, Messenger RNA; MTT, 3-(4,5-dimethylthiazol-2-yl)-2,5 diphenyltetrazolium bromide; NSCLC, Non-small cell lung cancer; PBS, phosphate buffer saline; PI, Propidium iodide; PVDF, Polyvinylidene fluoride; qRT-PCR, Quantitative real time-polymerase chain reaction; RIPA, Radio immunoprecipitation assay.

* Corresponding authors at: Department of Biochemistry and Molecular Biology, Faculty of Pharmacy (Boys), Al-Azhar University, Nasr City, Cairo 11651, Egypt.
E-mail addresses: MohamedElkady1565.el@azhar.edu.eg (M.A. Elkady), ahmed_doghish@azhar.edu.eg (A.S. Doghish).

Peer review under responsibility of King Saud University.

Production and hosting by Elsevier

https://doi.org/10.1016/j.sjbs.2021.02.001
1319-562X/

is hampered by lagging of knowledge regarding the molecular pathophysiology of LC (Ray et al., 2010).

Recently, the dysregulation of microRNAs (miRs or miRNAs) has been widely reported in LC (Wu et al., 2019). MiRNAs are a group of non-coding RNAs that function as gene silencers post-transcriptionally leading to translation repression of messenger RNA (mRNA) or mRNA degradation (Elshafei et al., 2017). MiRNAs are implicated in cancer development through targeting either oncogenes or tumor suppressor genes which intern regulate cell proliferation, cell cycle, and apoptosis (Zhou et al., 2017).

Previous computational analysis revealed a putative role of several miRNAs in NSCLC. Among the potential miRNAs which might be involved in NSCLC is miR-567 (Shao et al., 2017), which is encoded by the miR-567 gene located on chromosome 3q13.2 (El-Murr et al., 2012). In addition, several recent studies reported that miR-567 plays a decisive role in cancers as breast cancer (Bertoli et al., 2017; Han et al., 2020), osteosarcoma (Liu et al., 2018) and gastric cancer (Zhang et al., 2019).

Nevertheless, the role of miR-567 in NSCLC remains unexplored and need to be elucidated.

The plausible role of miR-567 is further substantiated by the previous findings that miR-567 regulates several cyclins, cyclin-dependent kinases (CDKs) affecting cell proliferation and cell cycle (Zhang et al., 2019). CDK8 as a member of CDKs is encoded by CDK8 gene located on chromosome 13q12.13 (Xu et al., 2015b). CDK8 was known as an oncogene that participated in regulating several cancer signaling pathways (Firestein et al., 2008; Alarcón et al., 2009). The CDK8 expression was found upregulated in breast carcinomas (Crown, 2017; McDermott et al., 2017), pancreatic cancer (Xu et al., 2015b), colorectal cancer (Ohtsuka et al., 2016), prostate cancer (Brägelmann et al., 2017; Nakamura et al., 2018), papillary thyroid carcinomas (Han et al., 2017) and glioma tissues (Zhang et al., 2018). But the expression pattern and function of CDK8 in NSCLC is unexplored until now.

Therefore, this study aimed to explore the potential regulatory role of miR-567 on the proliferation, cell cycle distribution, and apoptosis of A549 NSCLC cells and elucidate the possible associated molecular mechanism that may help in NSCLC treatment.

2. Materials and methods

2.1. Chemicals

Dimethyl sulfoxide (DMSO) and 3-(4,5-dimethylthiazol-2-yl)-2,5 diphenyltetrazolium bromide (MTT) were obtained from Sigma Aldrich (USA). 5-bromo- 2′-deoxyuridine (BrdU) was purchased from Invitrogen (TFS, USA, Catalog no. B23151). ß-Actin was obtained from Santa Cruz (USA, catalog no. sc-47778). Penicillin/streptomycin solution (Pen/Strep), Dulbecco's modified Eagle's medium (DMEM), fetal bovine serum (FBS), phosphate buffer saline (PBS), and trypsin- EDTA were purchased from Gibco (Gibco, TFS, USA). Radio immunoprecipitation assay (RIPA) lysis buffer (comprises of: 1% NP-40 or 1% Triton X-100, 150 mM NaCl, 0.1% SDS, 5 mM EDTA, 1% sodium deoxycholate, plus 25 mM Tris-HCl pH 7.6) was obtained from Sigma-Aldrich (USA).

2.2. Cell lines

Human bronchial epithelial (16HBE) normal cell line and A549, H460, and H1299 NSCLC cell lines were obtained from American type culture collection (ATCC; Manassas, VA, USA). All lines were maintained in DMEM containing 10% FBS and 1% Pen/Strep solution. Then, all cells were incubated at 37 °C in a humidified incubator with 5% CO_2. Growth and morphology were checked and cells were passaged when they had reached 80–90% confluence following trypsinization with 0.05% trypsin-EDTA.

2.3. MicroRNA transfection

A549 NSCLC cells were cultured in 6-well plates and incubated till 80–90% confluency and then divided into four groups; including A549 NSCLC cells were not transfected with any miRNA representing untransfected control group while the remaining A549 NSCLC cells were either transfected with mature miR-567 mimic (Syn-hsa-miR-567, QIAGEN, USA, catalog no. MIN0003231) representing miR-567 mimic group, miR-567 inhibitor (Anti-hsa-miR-567, QIAGEN, USA, catalog no. MSY0003231) representing miR-567 inhibitor group or negative control siRNA (AllStars Negative Control siRNA, QIAGEN, USA, catalog no. 1027280) representing negative control group via HiPerFect transfection reagent (QIAGEN, California, USA, catalog no. 301702) as manufacturer's guidelines and all wells were assigned for each group. Finally, all cultured cells were incubated for 72 h (h) and then collected for further post-transfection experiments (Huang et al., 2015).

2.4. Assessment of miR-567 and CDK8 mRNA expression

The relative expression of miR-567 in the cultured cells was assessed before and after transfection. Firstly, it was assessed before transfection to determine the potential roles of miR-567 in NSCLC cells as compared with normal 16HBE cell line. Secondly, the expression of miR-567 was evaluated after transfection to assess the successful transfection of miR-567 mimic and miR-567 inhibitor in A549 NSCLC cell line.

2.4.1. Total RNA isolation

Trizol reagent extraction method (Invitrogen, Germany, catalog no. 15596-026) was used to isolate total RNA from the cultivated cells. The isolated RNA pellets were treated with RNAse-free DNAse kit (Invitrogen, Germany). The RNA concentrations (ng/μL) and purities for all aliquots were determined using NanoDrop® 1000 spectrophotometer (Thermo Scientific, Wilmington, DE, USA). The isolated RNA aliquots were kept at −80 °C till the reverse transcription step.

2.4.2. Reverse transcription step

Complementary DNA (cDNA) was synthesized from isolated RNA using RevertAid™ First Strand cDNA Synthesis Kit (MBI Fermentas, Germany) according to the producer's directives using a thermocycler (Biometra GmbH, Göttingen, Germany), according to the following thermal program: the reverse transcription (RT) reaction was carried out at 25 °C for 10 min, followed by 1 h at 42 °C, and the reaction was stopped by heating for 5 min at 95 °C (Ismail et al., 2019). Afterward, the reaction tubes containing cDNA were collected on ice until being used for cDNA amplification.

2.4.3. Quantification of miR-567 and CDK8 mRNA using quantitative real time-polymerase chain reaction

A qRT-PCR was used to determine the cultured cell lines cDNA copy number. For detection of miRNA expression, amplifications were performed by using SYBR Green miScript Primer Assay for miR-567 (hsa-mir-567 miScript primer assay, Qiagen, USA, catalog no. 218300) on the basis of the manufacturer's guidelines. RNU6B (U6) small nuclear RNA was used as an internal control for data normalization. The qRT-PCR primers had the following sequences: Mature miR-567 (target): 5′-AGUAUGUUCUUCCAGGACAGAAC-3′; and RNU6B (reference): 5′-CGC AAG GAT GAC ACG CAA ATT CGT GAG CGT TCC ATATTTTT-3′. For detection of CDK8 mRNA expression, SYBR® Premix Ex Taq™ kit (TaKaRa, Biotech. Co. Ltd., China) was used in this step according to the manufacturer's instructions.

B-Actin was used as an internal control. The primer sequences used were as the following: for CDK8 (target) forward: 5′-GCCGGTTGT CAAATCCCTTAC-3′ and reverse: 5′-TGTGACTGCTGTCTTGATTCCCT-3′ and for B-Actin (reference) forward: 5′-TGGCACCCAGCACAAT GAA-3′ and reverse: 5′-CTAAGTCATAGTCCGCCTAGAAGCA-3′. The melting curve was obtained from 65℃ to 95 ℃. The relative expression of miR-567 and CDK8 mRNA to U6 and B-Actin respectively was calculated using the equation $2^{-\Delta Ct}$, where ΔCt = (CtmiR-567- CtU6) or ΔCt = (CtmRNA- CtB-actin). The fold change of miR-567 or CDK8 mRNA was determined by the $2^{-\Delta\Delta Ct}$ method.

2.5. Cell viability assay

Using MTT procedures, cell viability was assessed. The A549 NSCLC cells (5000 cells/well) were cultured in 96-well plates, transfected and incubated at 37 °C. After 24, 48, 72, and 96 h of incubation, 100 μL of MTT solution was added to wells (5 mg/ml in PBS) and maintained for 4 h at 37 °C. Then, 100 μL of DMSO (Sigma, USA) was added into each well to dissolve the formed formazan crystals. The plates were gently shaken on a swing bed for 10 min, and the optical density was measured at 570 nm by using a microplate reader (Epoc-2 C micro-plate reader, Bio Tek, VT, USA).

2.6. Cell proliferation assay

Using BrdU staining assay procedures, cell proliferation was assessed (Wang et al., 2016). The cells (2×10^5) for all groups were cultured, transfected and incubated in 6-well plates for 72 h, after that 10 μM BrdU labeling solution was added and incubated for 2 h. we get rid of BrdU labeling solution and cells were washed three times with PBS and fixed with 4% paraformaldehyde for 15 min at room temperature (RT). Afterward, a permeabilization buffer 0.3% Triton X-100 was added and incubated for 20 min at RT. Then 1 N HCl was added to the cells for 10 min on ice followed by 2 N HCl for 15 min at RT. Only 1 mL phosphate/citric acid buffer (pH 7.4) was added to wells and incubated for 10 min at RT. Then, the buffer was eliminated and anti-BrdU monoclonal primary antibody (Invitrogen, TFS, USA, catalog no. 14-5071-82) was applied and incubated at RT overnight. The incorporated BrdU was visualized by immunofluorescence through the addition of fluorescently labeled (peroxidase-conjugated) secondary antibody and incubated for 1 h at RT. DAPI (300 nM) was used for nuclear staining for 1 min in the dark at RT. Slides were mounted in fluoromount G and images of microscopic fields were taken using the LEICA fluorescence microscope (model: Leica DM5500 B from Leica Microsystems, USA). Fluorescence intensity of microscopic fields was measured using ImageJ/NIH software (National Institute of mental health, Bethesda, Maryland, USA) and the data were represented as a ratio red (Antibody fluorescence intensity) / blue (DAPI nuclei staining) (Pang et al., 2019).

2.7. Flow cytometric analysis of cell cycle

The effect of miR-567 mimic and inhibitor transfection on the cell cycle was investigated using propidium iodide (PI) staining and flow cytometric analysis using a cell cycle kit (PN C03551). In short, after cell transfection as previously mentioned for 72 h, A549 NSCLC cells were allowed to grow in a 25 cm^3 flask until 70–80% confluence was reached. Then we harvested the cells and make cell fixation by adding 1×10^6 cells in a 5 mL tube, centrifuged at 2000 rpm for 5 min and the supernatant was aspirated. The pellet of fixed cells was resuspended in 0.5 mL cell cycle kit, vortex, and incubated for 15 min at 25 °C away from light. Lastly, DNA was stained with 50 μg/mL propidium iodide for 30 min. Flow cytometric analysis of cell cycle performed on a COULTER ® EPICS ® XL™ Flow Cytometer (USA).

2.8. Flow cytometric analysis for detection of apoptosis

To examine the effect of miR-567 mimic and inhibitor transfection on cell apoptosis, Annexin V–FITC Kit was used along with the kit protocol (PN IM3546), followed by flow cytometric analysis. In brief, after cell transfection, as previously mentioned for 72 h, A549 NSCLC cells were allowed to grow in a 25 cm3 flask until 70–80% confluence was reached. After that, washed in PBS and suspended to 5×10^3–5×10^6 cells/mL in 1× binding buffer. Then we added to 100 μL of the cell suspensions, 5 μL of dissolved PI, and 1 μL of annexin V-FITC solution followed by incubation in the dark for 15 min. Next to that, we added 400 μL of ice-cold 1× binding buffer and mixed gently. Apoptotic cells were determined by flow cytometric analysis on a COULTER ® EPICS ® XL™ Flow Cytometer (USA).

2.9. Bioinformatics analyses

To predict the miR-567 possible target gene, three online software programs were used including TargetScan (http://www.targetscan.org/), miRDB (http://mirdb.org/miRDB/), and Diana Tools (http://diana.imis.athena-innovation.gr/DianaTools/). From the target genes obtained, we select genes that might contribute to the carcinogenesis of NSCLC.

2.10. Western blot analysis

The cultured A549 NSCLC cells for all groups were collected, washed with ice-cold PBS twice, and lysed by RIPA lysis buffer. The mixtures were sonicated, centrifuged and the supernatant was collected, divided into aliquots and total protein concentration for each sample was measured using the biuret method (Zheng et al., 2017; Mokhtar et al., 2020). Proteins in each sample were denatured at 95 °C for 5 min in 2× Laemmli buffer containing 5% β-mercaptoethanol. By loading equal amounts of protein (50 μg per lane) and separated by sodium dodecyl sulfate-polyacrylamide gel electrophoresis at 100 V through 6% stacking gel followed by 125 V via 10% resolving gel for approximately 2 h and then transferred to polyvinylidene fluoride (PVDF) membranes using semidry transfer unit (Cleaver Scientific, UK) for 25 min. Then, we blocked transferred PVDF membranes by incubation in TBS buffer containing 0.1% Tween and 5% defatted milk (TBST) for 1 h at 4 °C. Thereafter, membranes were incubated with rabbit polyclonal anti-cyclin-dependent kinase 8 (anti-CDK8) as the primary antibody (1:500, Elabscience Biotechnology, Inc., catalog no.E-AB-30870) overnight at 4 °C. Then, they were washed with TBST buffer and incubated for 1 h at RT with an alkaline phosphatase-conjugated goat anti-rabbit (1:5000, Novus Biologicals, LLC, Littleton, CO, USA) as the secondary antibody. Following four washes with TBST, the membrane-bound antibody specific bands were visualized by using BCIP/NBT substrate detection Kit (Genemed Biotechnologies, Inc., CA, USA), and the intensity of the bands was quantified by ImageJ/NIH software. Equivalent protein loading for each lane was confirmed by stripping and reblotting membranes at 4 °C against mouse monoclonal anti-ß-Actin antibody (1:500, Santa Cruz Biotechnology, USA, catalog no. sc-47778) (Elsadek et al., 2017; Ismail et al., 2020).

2.11. Statistical analysis

GraphPad Prism 6 software (GraphPad, San Diego, CA, USA) was used to analyze all results. The data were represented as mean ± standard deviation (Mean ± SD) from at least three independent experiments (n = 3). One-way analysis of variance (One-way ANOVA) followed by Tukey post hoc multiple comparison tests

were opted to analyze the significant difference between all groups' results. P < 0.05 was considered statistically significant.

3. Results

3.1. MiR-567 expression level is downregulated in the studied NSCLC cell lines as compared to normal 16HBE cell line

In the current study, we began with the assessment of the miR-567 expression levels in A549, H460, H1299 NSCLC cell lines, along with the normal 16HBE cell line before transfection to anticipate the possible role of miR-567 in NSCLC cells. Our qRT-PCR results found that miR-567 expression levels were decreased significantly in A549, H460, and H1299 cells as compared to the normal 16HBE cell line (Fig. 1). Since the A549 cell line showed the lowest miR-567 expression level ($P < 0.0001$); therefore, we opt to continue the rest of our study using this cell line.

3.2. MiR-567 mimic and miR-567 inhibitor are successfully transfected in A549 NSCLC cells

The qRT-PCR was used to confirm the successful transfection of miR-567 mimic and miR-567 inhibitor in A549 NSCLC cell line through evaluation of the miR-567 expression levels after its transfection with miR-567 mimic and miR-567 inhibitor. In this study, a significantly higher miR-567 expression level was observed in A549 cells transfected with miR-567 mimic as compared to both untransfected and negative control groups ($P < 0.0001$). In contrast, the miR-567 expression level decreased significantly in A549 cells transfected with miR-567 inhibitor when compared to untransfected and negative control groups ($P = 0.0005$ & $P = 0.0015$) (Fig. 2). These results confirmed that A549 NSCLC cells were successfully transfected with miR-567 mimic and miR-567 inhibitor.

3.3. MiR-567 overexpression inhibited A549 cell viability and proliferation

The MTT assay and BrdU assay methods were performed to explore the effect of miR-567 on viability and proliferation pattern of A549 cells after their transfection with miR-567 mimic and miR-567 inhibitor. Firstly, it was observed that A549 cell viability was inhibited significantly by miR-567 overexpression at 72 and 96 h post-transfection when compared to untransfected and negative control groups. Moreover, miR-567 overexpression significantly inhibited A549 cell viability at 48 h when compared only to the negative control. On the other hand, the A549 cell viability at 72 and 96 h after transfection was remarkably promoted by decrease the expression of miR-567 when compared to untransfected and negative control groups (Fig. 3 A).

Secondly, the BrdU assay results revealed that the A549 cell proliferation was suppressed by miR-567 overexpression when compared to untransfected and negative control groups ($P < 0.0001$). Whereas, miR-567 inhibitor transfection triggered A549 cell proliferation when compared to untransfected and negative control groups ($P < 0.0001$) (Fig. 3 B & C).

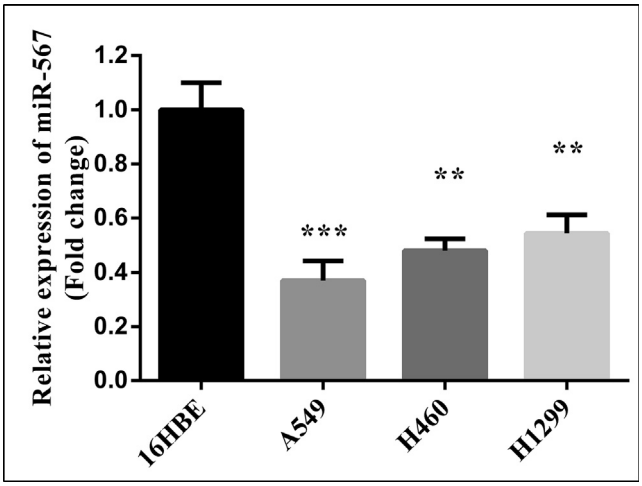

Fig. 1. MiR-567 relative expression reduced in A549, H460, and H1299 NSCLC cell lines as compared to 16HBE normal cell line detected by qRT-PCR. Data were presented as Mean ± SD from 3 independent experiments (n = 3). ** Significant $P < 0.001$ and *** significant $P < 0.0001$ from 16HBE cell line.

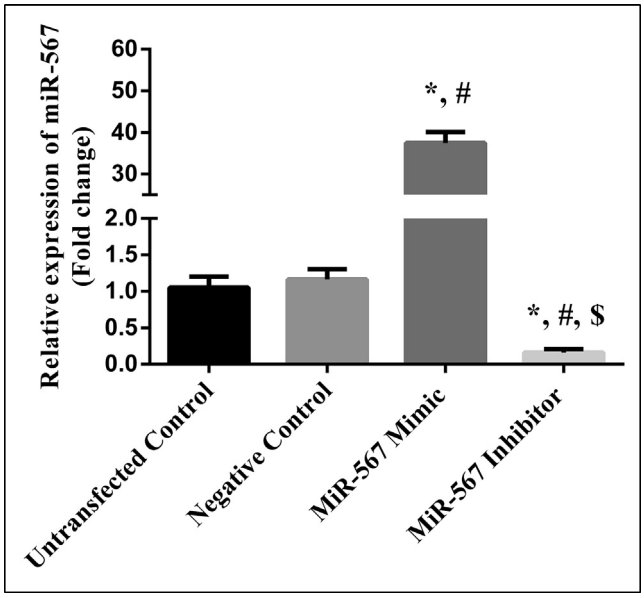

Fig. 2. A549 NSCLC cells were successfully transfected with miR-567 mimic and miR-567 inhibitor. Elevated miR-567 expression was observed post transfection with miR-567 mimic, and reduced expression post miR-567 inhibitor transfection in A549 NSCLC investigated by qRT-PCR. Data were presented as Mean ± SD from 3 independent experiments (n = 3). * Significant $P < 0.005$ from untransfected control, # significant $P < 0.005$ from negative control and **$** significant $P < 0.005$ from miR-567 mimic.

3.4. MiR-567 overexpression promoted cell apoptosis and suppressed A549 NSCLC cell cycle progression

The effect of miR-567 on A549 NSCLC cell growth and cell cycle distribution was examined 72 h after the transfection of A549 cells with miR-567 mimic, miR-567 inhibitor, and negative control siRNA by using flow cytometry. It was found that miR-567 overexpression significantly increased the accumulation of cells at both sub-G1 and S phases ($P < 0.0001$) and remarkably reduced the G1 phase cells ($P < 0.0001$) in A549 cells as compared to untransfected and negative control groups. So, the overexpression of miR-567 suppressed cell growth by arresting the A549 cells at sub-G1 and S phases. Furthermore, miR-567 downregulation significantly reduced the accumulation of cells at sub-G1 phase ($P = 0.0002$ & $P = 0.0001$) as compared to untransfected and negative control groups as illustrated in Fig. 4.

Moreover, After 72 h from transfection of A549 cells with miR-567 mimic, miR-567 inhibitor, and negative control siRNA, cell apoptosis was assessed. It was observed that miR-567 overexpression remarkably promoted cell apoptosis when compared to untransfected and negative control groups ($P < 0.0001$). In contrast,

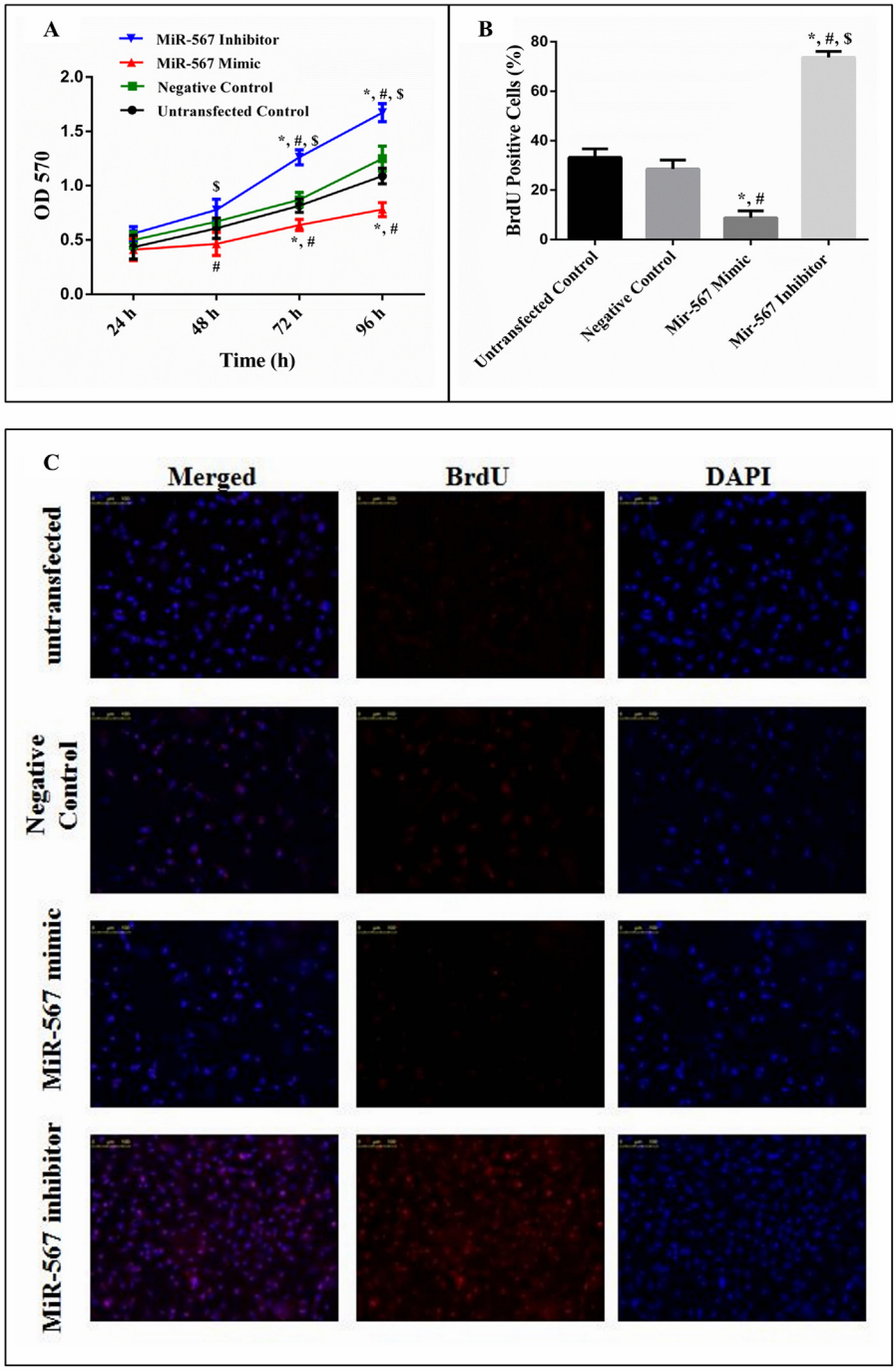

Fig. 3. MiR-567 upregulation suppressed A549 cell viability and cell proliferation whereas miR-567 inhibitor promoted A549 cell viability and cell proliferation evaluated by MTT assay (A) and BrdU assay (B) respectively. (C) BrdU-positive cells in all groups were analyzed by Image J software (Red/Blue). Scale bar, 20 μm. Data were expressed as Mean ± SD from 3 independent experiments (n = 3). *: significant $P < 0.005$ from untransfected control, #: significant $P < 0.005$ from negative control, and $: significant $P < 0.005$ from miR-567 mimic. BrdU: 5-bromo- 2′-deoxyuridine, MTT: 3-(4,5-dimethylthiazol-2-yl) −2,5 diphenyltetrazolium bromide and OD: optical density.

miR-567 downregulation remarkably reduced cell apoptosis as compared to untransfected and negative control groups ($P = 0.002$) (Fig. 5).

3.5. CDK8 was predicted as a supposed target of miR-567 by bioinformatics analysis programs

By using TargetScan, miRDB, and Diana Tools, we searched for miR-567 putative target gene to discover the possible underlying molecular mechanism of miR-567 involved in suppression of A549 NSCLC cell growth and proliferation. One of the best remarkable candidate genes highly expected to be targeted by miR-567 was the CDK8 gene that was reported to be associated with carcinogenesis of multiple cancers and still unexplored in NSCLC. It was found that there were two binding sites for miR-567 in the 3′-UTR of the CDK8 mRNA ranging from (412–429 bp) and from (1030–1041 bp) with binding type 7mer for each binding site (Fig. 6).

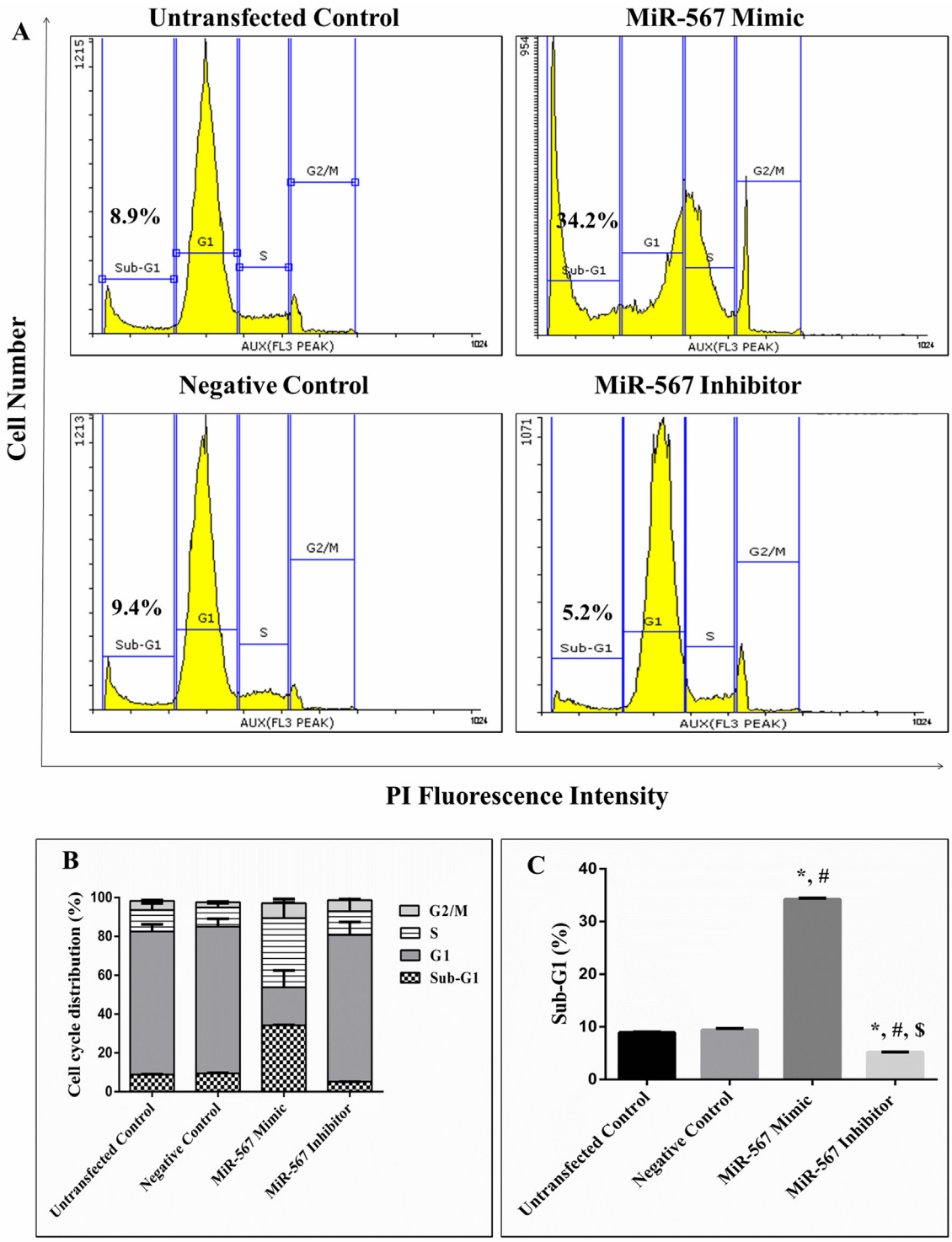

Fig. 4. MiR-567 overexpression remarkably suppressed cell cycle progression at both sub-G1 and S phases. (A) The histograms represented the proportion of cell distribution in different phases of cell cycle (Sub-G1, G1, S and G2/M) at 72 h post transfection of A549 cells with miR-567 mimic, inhibitor and negative control siRNA. (B) Cell cycle distributions in in all groups. (C) miR-567 overexpression remarkably increased cells at sub-G1 whereas miR-567 downregulation significantly reduced the sub-G1 phase cells. Data were expressed as Mean ± SD from 3 independent experiments (n = 3). * Significant $P < 0.005$ from untransfected control, # significant $P < 0.005$ from negative control, and $ significant $P < 0.005$ from miR-567 mimic. PI: Propidium iodide.

3.6. MiR-567 overexpression remarkably reduced the CDK8 expressions at both mRNA and protein levels in A549 cell line

To clarify the effect of miR-567 on CDK8 gene expression in A549 cells, the expression pattern of CDK8 gene at both mRNA and protein levels was examined 72 h post the transfection of A549 NSCLC cells with miR-567 mimic, and miR-567 inhibitor via qRT-PCR and western blotting. Firstly, The qRT-PCR results observed that the CDK8 mRNA expression level remarkably reduced in A549 cells post transfected with miR-567 mimic

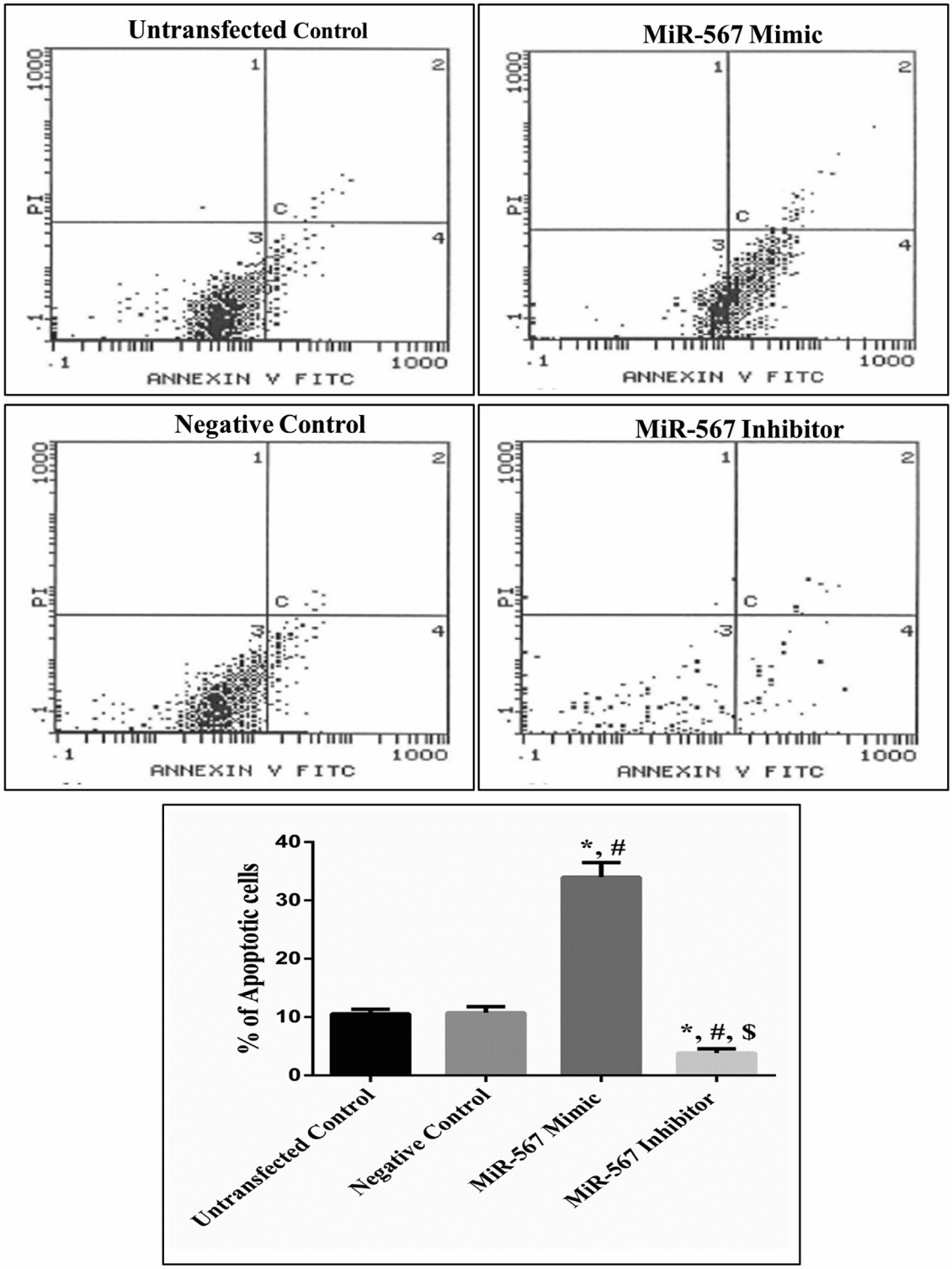

Fig. 5. MiR-567 overexpression triggered cell apoptosis in A549 NSCLC cells. MiR-567 mimic remarkably increased the ratio of apoptotic cells while miR-567 inhibitor remarkably reduced the ratio of apoptotic cells assessed by flow cytometry. Data were presented as Mean ± SD from 3 independent experiments (n = 3). * Significant $P < 0.005$ from untransfected control, **#** significant $P < 0.005$ from negative control, and **$** significant $P < 0.005$ from miR-567 mimic.

($P = 0.004$ & $P = 0.002$) and increased in A549 cells post transfected with miR-567 inhibitor ($P < 0.0001$) as compared to untransfected and negative control groups (Fig. 7).

Furthermore, the miR-567 overexpression reduced CDK8 protein levels ($P = 0.008$ & $P = 0.007$) while the miR-567 suppression elevated CDK8 protein levels ($P = 0.04$ & $P = 0.06$) when compared to untransfected and negative control groups that indicate a significant negative correlation between expression levels of miR-567 and CDK8 in A549 cells (Fig. 8 A & B).

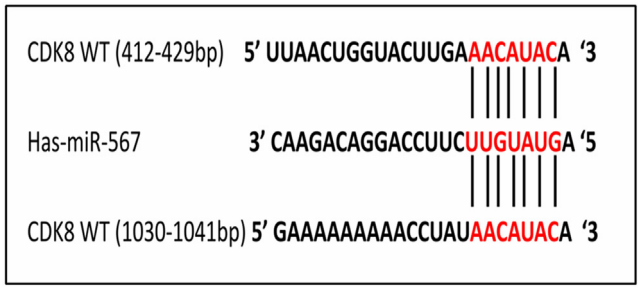

Fig. 6. CDK8 is a possible target of miR-567. Two predicted binding sites for miR-567 on the 3′ UTR of human wild-type CDK8 mRNA ranging from (412 to 429 bp) and from (1030 to 1041 bp) with binding type 7mer for both binding sites. CDK8: Cyclin-dependent kinase 8.

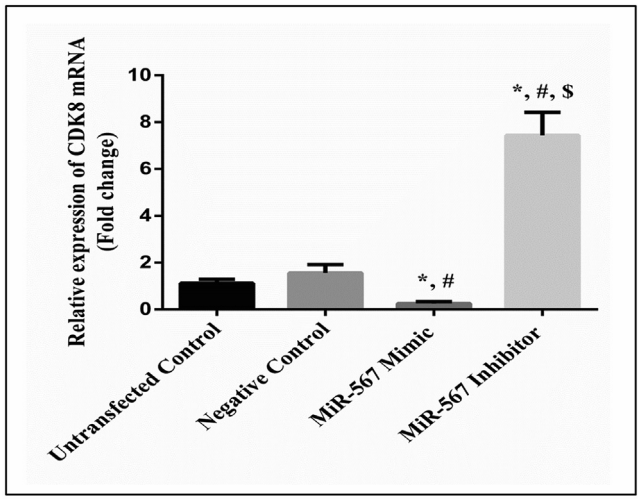

Fig. 7. MiR-567 overexpression suppressed CDK8 mRNA expression level. MiR-567 mimic reduced CDK8 mRNA level in A549 NSCLC cells which elevated in A549 cells transfected with miR-567 inhibitor evaluated by qRT-PCR. Data were expressed as Mean ± SD from 3 independent experiments (n = 3). *Significant $P < 0.005$ from untransfected control, # significant $P < 0.005$ from negative control, and $ significant $P < 0.005$ from miR-567 mimic, CDK8: Cyclin-dependent kinase 8.

4. Discussion

Lung cancer is the highest recurrently diagnosed cancer throughout the world (Bray et al., 2018). In Egypt, the most prevalent cancers in males were liver, bladder, non-Hodgkin's lymphoma, and lung representing 50.6% of all reported cases of cancer in males (Ibrahim et al., 2014). Regrettably, the NSCLC patients are commonly discovered in late stages associated with poor prognosis and with a high mortality rate (Luo and Liang, 2018). Therefore, there is a pressing need to identify a new molecular mechanism that may enhance the NSCLC patients' prognosis and may help in NSCLC treatment.

Accumulating evidences revealed that the deviant expression of miRNAs participated in cancer progression by targeting either tumor-suppressive genes or oncogenes. For that reason, miRNAs can be recognised as oncogenes or tumor suppressors (Zhang et al., 2007; Skrzypski et al., 2011). The biological role of miR-567 in NSCLC either as an oncogene or a tumor suppressor remains unexplored. Based on integrative bioinformatics analysis, only one computational analysis predicted that miR-567 could be a putative biomarker for NSCLC (Shao et al., 2017). For that reason, in our study, we explored the role of miR-567 in NSCLC cells and elucidated its possible associated molecular mechanism in NSCLC treatment.

In the current study, we started firstly by examining the expression pattern of miR-567 in NSCLC cells as well as normal 16 HBE cells to expect the possible role of miR-567 in NSCLC cells. Interestingly, the results of this study revealed that miR-567 was remarkably decreased in all the studied NSCLC cell lines as compared to the normal 16HBE cell line. This result suggested that miR-567 might be a tumor suppressor for NSCLC cells and might be a new biomarker for NSCLC.

Aberrant cell proliferation and deviations in the cell cycle are essential elements of cancer (Hanahan and Weinberg, 2000; Wang et al., 2011). Our experimental analysis found that miR-567 upregulation significantly inhibited the NSCLC cell viability and cell proliferation whereas miR-567 downregulation significantly promoted NSCLC cell viability and proliferation. These findings indicated that miR-567 might be a tumor suppressor for NSCLC cells. Lately, another study supporting our findings and found that miR-567 functions as a tumor suppressor by preventing the proliferation of gastric cancer cells (Zhang et al., 2019). In addi-

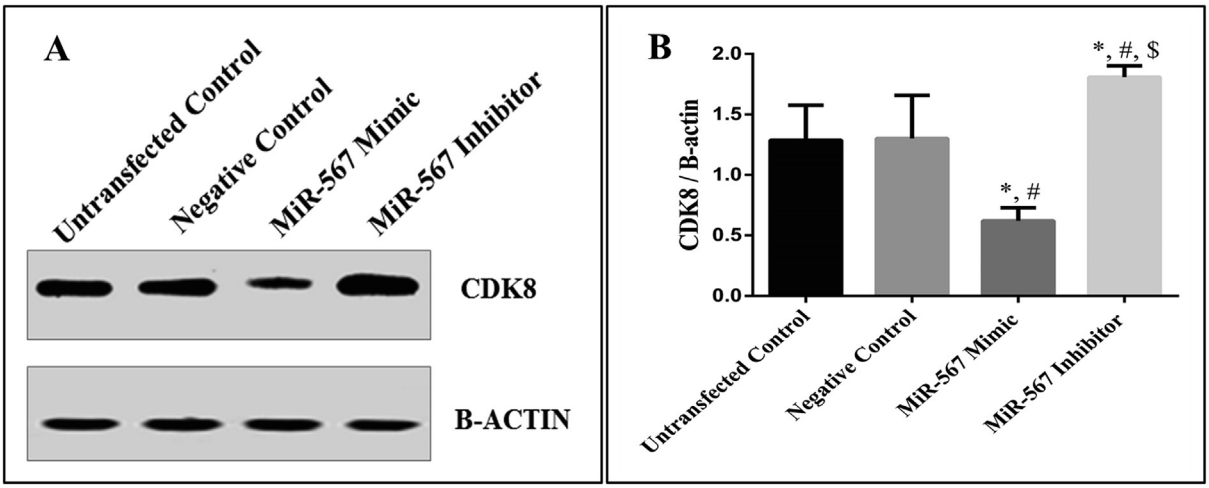

Fig. 8. MiR-567 overexpression suppressed CDK8 gene expression at protein level. (A) Western blot analyses of CDK8 protein levels in A549 NSCLC cells of different groups were analyzed by ImageJ software. (B) miR-567 mimic decreased CDK8 protein expression in A549 cells which was elevated post transfected with miR-567 inhibitor. Data were expressed as Mean ± SD from 3 independent experiments (n = 3) and expressed as relative to β-actin. *Significant $P < 0.005$ from untransfected control, # significant $P < 0.005$ from negative control, and $ significant $P < 0.005$ from miR-567 mimic, CDK8: Cyclin-dependent kinase 8.

tion, our results were consistent with Liu et al. who documented a suppression in osteosarcoma cell proliferation by miR-567 upregulation indicating its function as a tumor suppressor (Liu et al., 2018).

The cell cycle is comprised of different phases including Gap 1 (G1) phase, synthesis of DNA (S) phase, Gap 2 (G2) phase, and mitosis (M) phase while sub-G1 is cell cycle resting phase (Chulu and Liu, 2009). Interestingly, our results presented that miR-567 upregulation remarkably increased cell population at both sub-G1 and S phases and remarkably reduced cell population at G1 phase whereas miR-567 downregulation remarkably reduced the cell population at sub-G1 phase of the cell cycle in A549 NSCLC cells. So, the present findings proposed that miR-567 overexpression suppresses A549 NSCLC cell growth by the accumulation of cell population at both sub-G1 and S phases inducing cell cycle arrest. These results also suggested that miR-567 might be a tumor suppressor for A549 NSCLC. Furthermore, it was noted that miR-567 overexpression remarkably stimulated cell apoptosis while the downregulation of miR-567 remarkably reduced cell apoptosis in A549 NSCLC cells. Thus, these intriguing findings strongly proposed that miR-567 in A549 NSCLC cells could be a tumor suppressor.

Cyclins and CDKs are two core protein groups involved in cell cycle and cell proliferation control (Murray, 2004). Their dysregulation can disrupt normal cell differentiation, proliferation, cell cycle, and apoptosis leading to diseases and cancers (Malumbres and Barbacid, 2001; Wang et al., 2011). CDK8 was recognized as an oncogene that inhibits apoptosis and aberrant CDK8 expression is usually associated with tumorigeneses of cancers (Xu et al., 2015a). In the present study, the bioinformatics target analysis clarified that CDK8 was a target gene of miR-567. The miRDB program predicted CDK8 was miR-567 target gene with target score 100 and with two miR-567 binding sites in 3′-UTR of the CDK8 mRNA at (412–429 bp) and (1030–1041 bp) with binding type 7mer for both binding sites. Whereas TargetScan and Diana Tools anticipated CDK8 is a target for miR-567 with score 95 and miTG score 0.954 respectively with also two miR-567 binding sites in CDK8 mRNA 3′-UTR. These results strongly confirmed that CDK8 is a target gene of miR-567.

The CDK8 gene was reported to be associated with carcinogenesis of multiple cancers however its biological behavior in NSCLC still unexplored. To clarify this speculation, we evaluated the expression of CDK8 gene at both mRNA and protein levels after overexpression and downregulation of miR-567 in A549 NSCLC cells. Interestingly, our results revealed that the overexpression of miR-567 remarkably reduced the expression level of CDK8 mRNA whereas the downregulation of miR-567 remarkably increased the CDK8 mRNA expression. Likewise, miR-567 overexpression reduced CDK8 protein levels while the miR-567 suppression elevated CDK8 protein levels. These findings proposed that CDK8 is a target of miR-567 and there was a negative correlation observed between expression levels of miR-567 and CDK8 in A549 NSCLC cells.

Finally, our study found that miRNA-567 overexpression inhibited A549 NSCLC cell viability, proliferation, induced cell cycle arrest, and cell apoptosis via regulation of CDK8. These intriguing findings strongly indicated that miR-567 in NSCLC cells could be a tumor suppressor by regulating the CDK8 gene expression. However, patients' tissue samples data about miR-567 expression levels from NSCLC tissue and neighboring normal tissues are warranted in a future study to ensure the matching between the expression pattern of miR-567 in NSCLC tissues and cell lines that complete the picture about the regulatory role of miR-567 on NSCLC disease.

5. Conclusions

In summary, our study found that miR-567 affects the biological behavior of A549 NSCLC cells. MiR-567 overexpression inhibited A549 NSCLC cell proliferation, triggered cell apoptosis, and induced cell cycle arrest at both sub-G1 and S phases through downregulation of CDK8 mRNA and protein expression. These results clarified a tumor suppressor activity of miR-567 in A549 NSCLC cells. Thus, our findings may promote the use of miR-567 as a new therapeutic target for NSCLC treatment.

Funding

This research did not receive any specific grant from funding agencies in the public, commercial, or not-for-profit sectors.

CRediT authorship contribution statement

Mohamed A. Elkady: Conceptualization, Data curation, Formal analysis, Methodology, Supervision, Writing - original draft. **Ahmed S. Doghish:** Conceptualization, Data curation, Formal analysis, Methodology, Supervision, Writing - original draft. **Ahmed Elshafei:** Conceptualization, Methodology, Visualization, Validation, Investigation. **Mostafa M. Elshafey:** Conceptualization, Methodology, Project administration.

Declaration of Competing Interest

The authors declare that they have no known competing financial interests or personal relationships that could have appeared to influence the work reported in this paper.

Acknowledgments

The authors would like to thank Dr. Mohammad Helmy Rashed, Pharmacology and Toxicology Department, Faculty of Pharmacy (Boys), Al-Azhar University, for continuous help to complete the practical part. Finally, the authors would like to thank the Biochemistry and Molecular Biology Department, Faculty of Pharmacy (Boys), Al-Azhar University, Cairo, Egypt, for the great help and for providing the lab facilities.

References

Alarcón, C., Zaromytidou, A.-I., Xi, Q., Gao, S., Yu, J., Fujisawa, S., Barlas, A., Miller, A. N., Manova-Todorova, K., Macias, M.J., 2009. Nuclear CDKs drive Smad transcriptional activation and turnover in BMP and TGF-β pathways. Cell 139, 757–769.

Bertoli, G., Cava, C., Diceglie, C., Martelli, C., Rizzo, G., Piccotti, F., Ottobrini, L., Castiglioni, I., 2017. MicroRNA-567 dysregulation contributes to carcinogenesis of breast cancer, targeting tumor cell proliferation, and migration. Breast Cancer Res. Treat. 161, 605–616.

Brägelmann, J., Klümper, N., Offermann, A., Von Maessenhausen, A., Böhm, D., Deng, M., Queisser, A., Sanders, C., Syring, I., Merseburger, A.S., 2017. Pan-cancer analysis of the Mediator complex transcriptome identifies CDK19 and CDK8 as therapeutic targets in advanced prostate cancer. Clin. Cancer Res. 23, 1829–1840.

Bray, F., Ferlay, J., Soerjomataram, I., Siegel, R.L., Torre, L.A., Jemal, A., 2018. Global cancer statistics 2018: GLOBOCAN estimates of incidence and mortality worldwide for 36 cancers in 185 countries. CA Cancer J. Clin. 68, 394–424.

Chulu, J.L., Liu, H.J., 2009. Recent patents on cell cycle regulatory proteins. Recent Pat. Biotechnol. 3, 1–9.

Crown, J., 2017. CDK8: a new breast cancer target. Oncotarget 8, 14269–14270.

El-Murr, N., Abidi, Z., Wanherdrick, K., Svrcek, M., Gaub, M.-P., Flejou, J.-F., Hamelin, R., Duval, A., Lesuffleur, T., 2012. MiRNA genes constitute new targets for microsatellite instability in colorectal cancer. PLoS ONE 7, e31862.

Elsadek, B., Mansour, A., Saleem, T., Warnecke, A., Kratz, F., 2017. The antitumor activity of a lactosaminated albumin conjugate of doxorubicin in a chemically induced hepatocellular carcinoma rat model compared to sorafenib. Digestive Liver Dis. 49, 213–222.

Elshafei, A., Shaker, O., Abd El-motaal, O., Salman, T., 2017. The expression profiling of serum miR-92a, miR-375, and miR-760 in colorectal cancer: An Egyptian study. Tumor Biol. 39 (6), 1–14.

Firestein, R., Bass, A.J., Kim, S.Y., Dunn, I.F., Silver, S.J., Guney, I., Freed, E., Ligon, A.H., Vena, N., Ogino, S., 2008. CDK8 is a colorectal cancer oncogene that regulates β-catenin activity. Nature 455, 547–551.

Han, C., Zheng, W., Ge, M., Wang, K., Xiang, Y., Wang, P., 2017. Downregulation of cyclin-dependent kinase 8 by microRNA-148a suppresses proliferation and invasiveness of papillary thyroid carcinomas. Am. J. Cancer Res. 7 (10), 2081–2090.
Han, M., Hu, J., Lu, P., Cao, H., Yu, C., Li, X., Qian, X., Yang, X., Yang, Y., Han, N., 2020. Exosome-transmitted miR-567 reverses trastuzumab resistance by inhibiting ATG5 in breast cancer. Cell Death Dis. 11, 1–15.
Hanahan, D., Weinberg, R.A., 2000. The hallmarks of cancer. Cell 100 (1), 57–70.
Huang, H., Zhu, Y., Li, S., 2015. MicroRNA-122 mimic transfection contributes to apoptosis in HepG2 cells. Mol. Med. Rep. 12, 6918–6924.
Ibrahim, A.S., Khaled, H.M., Mikhail, N.N., Baraka, H., Kamel, H., 2014. Cancer incidence in egypt: results of the national population-based cancer registry program. J. Cancer Epidemiol 2014 (437971), 1–18.
Ismail, A., Abulsoud, A.I., Mansour, O.A., Fawzy, A., 2019. Diagnostic significance of miR-639 and miR-10b in breast cancer patients. Meta Gene 19, 155–159.
Ismail, A., Doghish, A.S., Elsadek, B.E., Salama, S.A., Mariee, A.D., 2020. Hydroxycitric acid potentiates the cytotoxic effect of tamoxifen in MCF-7 breast cancer cells through inhibition of ATP citrate lyase. Steroids 108656, 1–10.
Krishnamoorthy, V., Vilwanathan, R., 2020. Silencing Sirtuin 6 induces cell cycle arrest and apoptosis in non-small cell lung cancer cell lines. Genomics 112, 3703–3712.
Lemjabbar-Alaoui, H., Hassan, O.U., Yang, Y.-W., Buchanan, P., 2015. Lung cancer: Biology and treatment options. BBA 1856, 189–210.
Liu, D., Zhang, C., Li, X., Zhang, H., Pang, Q., Wan, A., 2018. MicroRNA-567 inhibits cell proliferation, migration and invasion by targeting FGF5 in osteosarcoma. EXCLI J. 17, 102–112.
Liu, J., Liu, S., Deng, X., Rao, J., Huang, K., Xu, G., Wang, X., 2019. MicroRNA-582-5p suppresses non-small cell lung cancer cells growth and invasion via downregulating NOTCH1. PLoS ONE 14.
Luo, H., Liang, C., 2018. MicroRNA-148b inhibits proliferation and the epithelial-mesenchymal transition and increases radiosensitivity in non-small cell lung carcinomas by regulating ROCK1. Exp. Therapeutic Med. 15, 3609–3616.
Malumbres, M., Barbacid, M., 2001. To cycle or not to cycle: a critical decision in cancer. Nat. Rev. Cancer 1, 222–231.
McDermott, M.S., Chumanevich, A.A., Lim, C.-U., Liang, J., Chen, M., Altilia, S., Oliver, D., Rae, J.M., Shtutman, M., Kiaris, H., 2017. Inhibition of CDK8 mediator kinase suppresses estrogen dependent transcription and the growth of estrogen receptor positive breast cancer. Oncotarget 8, 12558–12575.
Mokhtar, M.M., Khidr, E.G., Shaban, H.M., Allam, S., Elsadek, B.E., Salama, S.A., Ali, S. S., 2020. The effect of aryl hydrocarbon receptor ligands on gentamicin-induced nephrotoxicity in rats. Environ. Sci. Pollut. Res. 27, 1–14.
Murray, A.W., 2004. Recycling the cell cycle: cyclins revisited. Cell 116, 221–234.
Nakamura, A., Nakata, D., Kakoi, Y., Kunitomo, M., Murai, S., Ebara, S., Hata, A., Hara, T., 2018. CDK8/19 inhibition induces premature G1/S transition and ATR-dependent cell death in prostate cancer cells. Oncotarget 9, 13474–13487.
Ohtsuka, M., Ling, H., Ivan, C., Pichler, M., Matsushita, D., Goblirsch, M., Stiegelbauer, V., Shigeyasu, K., Zhang, X., Chen, M., Vidhu, F., Bartholomeusz, G.A., Toiyama, Y., Kusunoki, M., Doki, Y., Mori, M., Song, S., Gunther, J.R., Krishnan, S., Slaby, O., Goel, A., Ajani, J.A., Radovich, M., Calin, G.A., 2016. H19 Noncoding RNA, an Independent Prognostic Factor, Regulates Essential Rb-E2F and CDK8-β-Catenin Signaling in Colorectal Cancer. EBioMedicine 13, 113–124.
Pang, Y., Pan, L., Zhang, Y., Liu, G., 2019. TP53BP2 decreases cell proliferation and induces autophagy in neuroblastoma cell lines. Oncol. Lett. 17, 4976–4984.
Ray, M.R., Jablons, D., He, B., 2010. Lung cancer therapeutics that target signaling pathways: an update. Expert Rev. Respiratory Med. 4, 631–645.
Shao, Y., Liang, B., Long, F., Jiang, S.-J., 2017. Diagnostic microRNA biomarker discovery for non-small-cell lung cancer adenocarcinoma by integrative bioinformatics analysis. Biomed Res. Int. 2017 (2563085), 1–9.
Skrzypski, M., Dziadziuszko, R., Jassem, J., 2011. MicroRNA in lung cancer diagnostics and treatment. Mutation Res./Fundam. Mol. Mech. Mutagenesis 717, 25–31.
Wang, J., Wang, G., Ma, H., Khan, M.F., 2011. Enhanced expression of cyclins and cyclin-dependent kinases in aniline-induced cell proliferation in rat spleen. Toxicol. Appl. Pharmacol. 250, 213–220.
Wang, W., Chen, J., Dai, J., Zhang, B., Wang, F., Sun, Y., 2016. MicroRNA-16-1 inhibits tumor cell proliferation and induces apoptosis in A549 non-small cell lung carcinoma cells. Oncol. Res. Featuring Preclinical Clin. Cancer Therapeutics 24, 345–351.
Wu, K.-L., Tsai, Y.-M., Lien, C.-T., Kuo, P.-L., Hung, Jen, Y., 2019. The Roles of MicroRNA in Lung Cancer. Int. J. Mol. Sci. 20 (1611), 1–25.
Xu, D., Li, C.-F., Zhang, X., Gong, Z., Chan, C.-H., Lee, S.-W., Jin, G., Rezaeian, A.-H., Han, F., Wang, J., 2015a. Skp2–MacroH2A1–CDK8 axis orchestrates G2/M transition and tumorigenesis. Nat. Commun. 6, 1–14.
Xu, W., Wang, Z., Zhang, W., Qian, K., Li, H., Kong, D., Li, Y., Tang, Y., 2015b. Mutated K-ras activates CDK8 to stimulate the epithelial-to-mesenchymal transition in pancreatic cancer in part via the Wnt/β-catenin signaling pathway. Cancer Lett. 356, 613–627.
Yoshimura, A., Yamada, T., Miyagawa-Hayashino, A., Sonobe, Y., Imabayashi, T., Yamada, T., Okada, S., Shimamoto, T., Chihara, Y., Iwasaku, M., 2019. Comparing three different anti-PD-L1 antibodies for immunohistochemical evaluation of small cell lung cancer. Lung Cancer 137, 108–112.
Zhang, B., Pan, X., Cobb, G.P., Anderson, T.A., 2007. microRNAs as oncogenes and tumor suppressors. Dev. Biol. 302, 1–12.
Zhang, F., Li, K., Yao, X., Wang, H., Li, W., Wu, J., Li, M., Zhou, R., Xu, L., Zhao, L., 2019. A miR-567-PIK3AP1-PI3K/AKT-c-Myc feedback loop regulates tumour growth and chemoresistance in gastric cancer. EBioMedicine 44, 311–321.
Zhang, J.-F., Zhang, J.-S., Zhao, Z.-H., Yang, P.-B., Ji, S.-F., Li, N., Shi, Q.-D., Tan, J., Xu, X., Xu, C.-B., 2018. MicroRNA-770 affects proliferation and cell cycle transition by directly targeting CDK8 in glioma. Cancer Cell Int. 18 (195), 1–13.
Zhang, P., Shao, G., Lin, X., Liu, Y., Yang, Z., 2017. MiR-338-3p inhibits the growth and invasion of non-small cell lung cancer cells by targeting IRS2. Am. J. Cancer Res. 7 (1), 53–63.
Zheng, K., Wu, L., He, Z., Yang, B., Yang, Y., 2017. Measurement of the total protein in serum by biuret method with uncertainty evaluation. Measurement 112, 16–21.
Zhou, K., Liu, M., Cao, Y., 2017. New Insight into microRNA Functions in Cancer: Oncogene-microRNA-Tumor Suppressor Gene Network. Front. Mol. Biosci. 4. 46–46.
Zhu, D.-Y., Li, X.-N., Qi, Y., Liu, D.-L., Yang, Y., Zhao, J., Zhang, C.-Y., Wu, K., Zhao, S., 2016. MiR-454 promotes the progression of human non-small cell lung cancer and directly targets PTEN. Biomed. Pharmacother. 81, 79–85.